

Recent measurements of electroweak boson pair production of massive boson plus a photon and two jets from the CMS and ATLAS experiments

Ying An* on behalf of the ATLAS and CMS Collaborations

Deutsches Elektronen-Synchrotron in Hamburg, Germany

E-mail: ying.an@cern.ch

The latest results for measurements of electroweak (EW) boson pair production of $V\gamma$ ($V=W$ or Z) plus two jets (j) in LHC proton-proton collisions at a center-of-mass energy of 13 TeV are presented. The measurements are performed in final states of $\ell\ell\gamma jj$ and $\nu\nu\gamma jj$ in Z boson decay modes and $\ell\nu\gamma jj$ for W boson decay with the data recorded by the CMS and ATLAS detectors in 2016-2018 corresponding to integrated luminosities of 137 and 139 fb^{-1} . The inclusive or differential cross sections are measured with a large dijet mass required close to the phase space of the vector boson scattering (VBS) or fusion (VBF) process. Exclusion limits on anomalous quartic gauge couplings (aQGCs) based on the dimension eight operators of the effective field theory are derived at 95% confidence level. The upper limits of searches for a 125 GeV Higgs boson to invisible particles ($H \rightarrow \chi\chi$) and a dark photon ($H \rightarrow \gamma\gamma_d$) are set in the $Z(\nu\nu)\gamma jj$ measurement assuming the Standard Model (SM) production cross section.

The 11th annual conference on Large Hadron Collider Physics

22-27 May 2023

Faculty of Physics and Institute of Physics of the University of Belgrade, Belgrade, Serbia

*Speaker

1. Introduction

The VBS/F process, collectively referred to as VBS below, is of great interest and significance where the two vector bosons radiated from the incoming quarks scatter or fuse to produce new vector bosons leading to the two outgoing quarks which appear as jets (j). It thus has the kinematic features that the two jets tend to be in the forward regions of the detector and have high energy [1].

The VBS $V\gamma$ production profits from the larger cross section, so more precise measurements such as the differential cross sections could be carried out, which is a good platform not only for accurate SM tests but also a window for the beyond SM (BSM) scenarios including the aGCs at energy scales outside the current reach. Moreover, the presence of the photon leaves more possibilities for searching for the different BSM hypotheses.

2. The EW $Z\gamma jj$ production measurements

The EW $Z\gamma jj$ production is measured in final states of $Z \rightarrow \ell\ell$ ($\ell = e$ or μ) by both the CMS [2] and ATLAS [3] Collaborations [4, 5], and $Z \rightarrow \nu\nu$ by ATLAS [6, 7], in which the $\ell\ell\gamma jj$ measurement gives the first observation of the EW $Z\gamma jj$ production.

In the EW $\ell\ell\gamma jj$ measurement, the main backgrounds are the chromodynamics-induced (QCD) $Z\gamma jj$, misidentification of jets as photons, referred to as the nonprompt photon, $t\bar{t}\gamma$, and VV . The interference between EW and QCD production is considered as background and included in the QCD source in the CMS case but as a systematic uncertainty in the ATLAS case. The nonprompt contribution is estimated from data by so-called methods “template-fit” [5] and “ABCD” [8] in two experiments, respectively. Others are estimated from the corresponding simulation where the most important background QCD $Z\gamma+jets$ is simulated by the generator MADGRAPH5_AMC@NLO [9] and SHERPA [10] in the CMS and ATLAS cases, respectively.

To select the Z boson and reduce the contribution of the final state radiation (FSR), both the CMS and ATLAS measurements impose the invariant mass of the $\ell\ell$ and $\ell\ell\gamma$ systems. To define the signal region, similar requirements of $m_{jj} > 500$ GeV, $|\Delta\eta_{jj}| > 2.5$ ($|\Delta y| > 1.0$), $\eta^* < 2.4$ ($\zeta(Z\gamma) < 0.4$) [11] are used in the CMS (ATLAS) case, where $\eta^* = |\eta_{Z\gamma} - (\eta_{j1} + \eta_{j2})/2|$ and $\zeta(Z\gamma) = \left| \frac{y_{Z\gamma} - (y_{j1} + y_{j2})/2}{\Delta y_{jj}} \right|$. To define the control region, the requirement of $150 < m_{jj} < 500$ GeV ($\zeta(Z\gamma) > 0.4$) is used in the CMS (ATLAS) case. In the signal region, requirements of $\Delta\phi_{Z\gamma, jj} = |\phi_{Z\gamma} - \phi_{j1j2}| > 1.9$ and $N_j^{\text{gap}} = 0$ [4] are further applied in two measurements. By utilizing the maximum likelihood fit [12] simultaneously for events in both the SR and CR, the inclusive and differential cross sections for EW and EW+QCD are measured in both the CMS and ATLAS measurements. Post-fit results in the SR in distributions of m_{jj} are shown in Fig. 1 (left and center).

In the EW $\nu\nu\gamma jj$ measurement, the signature of signals comprises moderate missing transverse (E_T^{miss}), a photon, and a pair of forward jets. Results are measured separately in two different photon energy ranges of $15 < p_T^\gamma < 110$ GeV [6] and $p_T^\gamma > 150$ GeV [7]. The latter benefits from the QGC contribution. Since the Z boson could be barely selected, the irreducible background in this situation thus includes additional $W\gamma+jets$ production besides the QCD $Z\gamma+jets$ production. The contribution from $t\bar{t}\gamma$ and VV production is small due to the lack of leptons. For the contribution from misidentification estimated by data, both jets misidentified as photons and electrons misidentified as photons [14] are needed. For separating signal and background further, a variable $C_\gamma =$

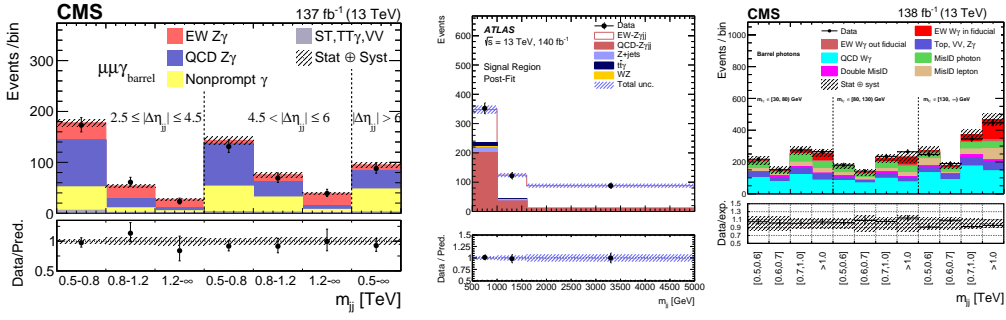


Figure 1: Post-fit results in distributions of m_{jj} for productions of EW $Z(\ell\ell)\gamma jj$ (left and center) and EW $W\gamma jj$ (right) [4, 5, 13].

$\exp\left[-\frac{4}{(\eta_{j1}-\eta_{j2})^2}(\eta_\gamma \frac{\eta_{j1}+\eta_{j2}}{2})^2\right]$ [15] is defined which varies from 0 to 1 corresponding to the photon out of and in the center of two VBS jets. Another variable C_3 is obtained, if replace η_γ to η_{j3} . The SR events are required to pass $C_\gamma > 0.4$ and $C_3 < 0.7$ due to $C_\gamma \approx 0.4$ when the photon aligns with one of the VBS jets. To constrain the normalization and validate the modelling of the main backgrounds, a $Z\gamma$ CR dominated by the QCD $Z\gamma$ +jets contribution is defined by requiring $C_\gamma < 0.4$. Two $W\gamma$ CRs are defined according to the lepton flavour with merely the same kinematic selection as the SR except for allowing lepton existence as well as removing E_T^{miss} requirement. Simultaneous maximum likelihood fit is used in bins of m_{jj} and boost decision tree (BDT) [16] distributions for $15 < p_T^\gamma < 110$ GeV and $p_T^\gamma > 150$ GeV corresponding to the observed (expected) significance 5.2 (5.1) and 3.2 (3.7) standard deviations.

3. The EW $W\gamma jj$ production measurement

The EW $W\gamma jj$ production is measured via the W boson leptonic decay by the CMS experiment based on both the 2016 and full Run 2 data [13, 17]. The former gave the first observation and the latter provided precise differential cross sections.

In the EW $\ell\nu\gamma jj$ measurement, events of interest have exactly one lepton, at least one photon and two jets. To reduce multijet contribution, the basic selection is $m_T^W > 30$ GeV and $p_T^{\text{miss}} > 30$ GeV, where $m_T^W = \sqrt{2p_T^\ell p_T^{\text{miss}} [1 - \cos(\Delta\phi_{\ell, p_T^{\text{miss}}})]}$. The source of backgrounds in this measurement contains the contribution from jets misidentified as leptons, referred to as nonprompt lepton, except for the nonprompt photon contribution, estimated by the ‘‘tight-to-loose’’ method [18]. Other backgrounds are the QCD $W\gamma jj$, $t\bar{t}\gamma$, VV , and $Z\gamma$ productions, in which the $Z\gamma$ contribution in the electron channel is largely suppressed by the requirement of $|m_{e\gamma} - m_Z| > 10$ GeV. What’s more, the double misidentification is also added properly.

The signal region (SR) is defined with the additional requirements of $m_{jj} > 500$ GeV, $|\Delta\eta_{jj}| > 2.5$, $m_{W\gamma} > 100$ GeV, $|y_{W\gamma} - (y_{j1} + y_{j2})/2| < 1.2$ [11], and $\Delta\phi_{W\gamma, jj} = |\phi_{W\gamma} - \phi_{j1j2}| > 2$, where variables in the $W\gamma$ system are built from the estimation of the longitudinal component of the neutrino momentum referred to Ref. [19, 20]. The CR is with requirement $200 < m_{jj} < 400$ GeV. Results are extracted by performing a binned likelihood fit to the data of the two-dimensional (2D) distribution in m_{jj} and $m_{\ell\gamma}$, signal significance, inclusive and differential cross sections for both EW and EW+QCD are calculated. Fig. 1 (right) shows the post-fit result of significance measurement.

4. The BSM search in the VBS $V\gamma$ process

For VBS $V\gamma$ production, the new physics BSM could induce aGCs which enlarges the cross section. The effect could be described using the effective theory (EFT) [21] linearly parameterised Lagrangian as follows:

$$\mathcal{L}_{EFT} = \mathcal{L}_{SM} + \sum_i \frac{c_i^{(6)}}{\Lambda^2} \mathcal{O}^{(6)} + \frac{c_i^{(8)}}{\Lambda^4} \mathcal{O}^{(8)} + \dots, \quad (1)$$

where $\mathcal{O}^{(n)}$ is dimension- n operators [22] induced by integrating out the new degrees of freedom, c_i is the corresponding coefficient, and Λ is a mass-dimension parameter related to the energy scale of the $\mathcal{O}^{(n)}$ operators. The VBS $V\gamma$ process is more sensitive to aQGCs than aTGCs and any aGCs could lead to the large invariant mass in the $V\gamma$ system. Limits on the dimension-8 operator coefficients are then derived using test statistics based on the profile likelihood ratio with a large value for p_T^γ . Fig. 2 shows the post-fit $m_{V\gamma}$ distribution with the number of events in the case of a non-zero EFT coefficient set. The constraints are either competitive with or more stringent than those previously published results [23, 24].

For the measurement of EW $Z(\nu\nu)\gamma jj$ with low p_T^γ requirement, searches for the Higgs boson to invisible particles (χ) and a dark photon (γ_d) are performed. The observed (expected) branching upper limit for the Higgs boson to invisible particles is 0.37 (0.34 $^{+0.15}_{-0.14}$) at 95% confidence level. The observed (expected) $H \rightarrow \gamma\gamma_d$ branching ratio upper limit is 0.018 (0.017 $^{+0.007}_{-0.005}$) at 95% CL when $m_H = 125$ GeV. The limits are also interpreted on $\sigma_{VBF} \times \mathcal{B}(H \rightarrow \gamma\gamma_d)$ for different Higgs mass hypotheses ranging from 60 GeV to 2 TeV.

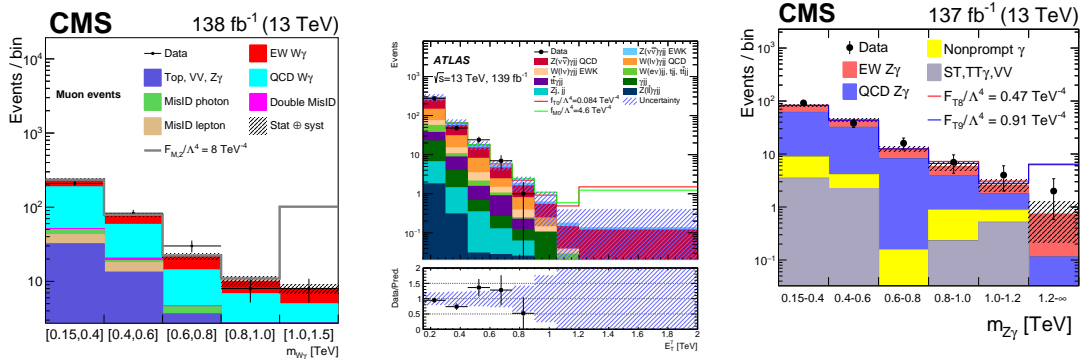


Figure 2: Post-fit results in distributions of mass or energy in $V\gamma$ system for productions of EW $W\gamma jj$ (right), EW $Z(\nu\nu)\gamma jj$ (center), and EW $Z(\ell\ell)\gamma jj$ (left) with the histogram of non-zero EFT coefficient [5, 7, 13].

5. Conclusion

The recent VBS $V\gamma$ measurements from the CMS and ATLAS experiments are introduced. The CMS reports the first observations of the EW $Z\gamma jj$ and $W\gamma jj$ production. The ATLAS provides the first EW $Z\gamma jj$ measurement in $Z \rightarrow \nu\nu$ decay mode. Plenty of BSM searches are performed including limits for the aQGC and rare Higgs decay branching ratio.

References

- [1] M. Rauch, *Vector-Boson Fusion and Vector-Boson Scattering*, [1610.08420](#).
- [2] CMS Collaboration, *The CMS Experiment at the CERN LHC*, *JINST* **3** (2008) S08004.
- [3] ATLAS Collaboration, *The ATLAS Experiment at the CERN Large Hadron Collider*, *JINST* **3** (2008) S08003.
- [4] ATLAS Collaboration, *Measurement of the cross-sections of the electroweak and total production of a $Z\gamma$ pair in association with two jets in pp collisions at $\sqrt{s} = 13$ TeV with the ATLAS detector*, *Phys. Lett. B* **846** (2023) 138222 [[2305.19142](#)].
- [5] CMS Collaboration, *Measurement of the electroweak production of $Z\gamma$ and two jets in proton-proton collisions at $\sqrt{s} = 13$ TeV and constraints on anomalous quartic gauge couplings*, *Phys. Rev. D* **104** (2021) 072001 [[2106.11082](#)].
- [6] ATLAS Collaboration, *Observation of electroweak production of two jets in association with an isolated photon and missing transverse momentum, and search for a Higgs boson decaying into invisible particles at 13 TeV with the ATLAS detector*, *Eur. Phys. J. C* **82** (2022) 105 [[2109.00925](#)].
- [7] ATLAS Collaboration, *Measurement of electroweak $Z(\nu\bar{\nu})\gamma jj$ production and limits on anomalous quartic gauge couplings in pp collisions at $\sqrt{s} = 13$ TeV with the ATLAS detector*, *JHEP* **06** (2023) 082 [[2208.12741](#)].
- [8] ATLAS Collaboration, *Electron reconstruction and identification in the ATLAS experiment using the 2015 and 2016 LHC proton-proton collision data at $\sqrt{s} = 13$ TeV*, *Eur. Phys. J. C* **79** (2019) 639 [[1902.04655](#)].
- [9] J. Alwall, R. Frederix, S. Frixione, V. Hirschi, F. Maltoni, O. Mattelaer et al., *The automated computation of tree-level and next-to-leading order differential cross sections, and their matching to parton shower simulations*, *JHEP* **07** (2014) 079 [[1405.0301](#)].
- [10] E. Bothmann, G.S. Chahal, S. Höche, J. Krause, F. Krauss, S. Kuttimalai et al., *Event generation with Sherpa 2.2*, *SciPost Phys.* **7** (2019) 034.
- [11] D. Rainwater, R. Szalapski and D. Zeppenfeld, *Probing color singlet exchange in $Z+2$ -jet events at the CERN LHC*, *Phys. Rev. D* **54** (1996) 6680 [[hep-ph/9605444](#)].
- [12] G. Cowan, K. Cranmer, E. Gross and O. Vitells, *Asymptotic formulae for likelihood-based tests of new physics*, *Eur. Phys. J. C* **71** (2011) 1554 [[1007.1727](#)].
- [13] CMS Collaboration, *Measurement of the electroweak production of $W\gamma$ in association with two jets in proton-proton collisions at $\sqrt{s} = 13$ TeV*, *Phys. Rev. D* **108** (2023) 032017 [[2212.12592](#)].

- [14] ATLAS Collaboration, *Search for dark matter at $\sqrt{s} = 13$ TeV in final states containing an energetic photon and large missing transverse momentum with the ATLAS detector*, *Eur. Phys. J. C* **77** (2017) 393 [1704.03848].
- [15] ATLAS Collaboration, *Observation and measurement of Higgs boson decays to WW^* with the ATLAS detector*, *Phys. Rev. D* **92** (2015) 012006 [1412.2641].
- [16] T. Chen and C. Guestrin, *Xgboost: A scalable tree boosting system*, .
- [17] CMS Collaboration, *Observation of electroweak production of $W\gamma$ with two jets in proton-proton collisions at $\sqrt{s} = 13$ TeV*, *Phys. Lett. B* **811** (2020) 135988 [2008.10521].
- [18] CMS Collaboration, *Observation of electroweak production of same-sign W boson pairs in the two jet and two same-sign lepton final state in proton-proton collisions at $\sqrt{s} = 13$ TeV*, *Phys. Rev. Lett.* **120** (2018) 081801 [1709.05822].
- [19] Particle Data Group, M. Tanabashi et al., *Review of particle physics*, *Phys. Rev. D* **98** (2018) 030001.
- [20] CMS Collaboration, *Search for a heavy resonance decaying to a pair of vector bosons in the lepton plus merged jet final state at $\sqrt{s} = 13$ TeV*, *JHEP* **05** (2018) 088 [1802.09407].
- [21] C. Degrande, N. Greiner, W. Kilian, O. Mattelaer, H. Mebane, T. Stelzer et al., *Effective Field Theory: A Modern Approach to Anomalous Couplings*, *Annals Phys.* **335** (2013) 21 [1205.4231].
- [22] O.J.P. Eboli, M.C. Gonzalez-Garcia and J.K. Mizukoshi, *$p p \rightarrow jj e^+ \mu^+ \nu \nu$ and $jj e^+ \mu^- \nu \nu$ at $O(\alpha(\text{em})^6)$ and $O(\alpha(\text{em})^4 \alpha(s)^2)$ for the study of the quartic electroweak gauge boson vertex at CERN LHC*, *Phys. Rev. D* **74** (2006) 073005 [hep-ph/0606118].
- [23] CMS Collaboration, *Search for anomalous electroweak production of vector boson pairs in association with two jets in proton-proton collisions at 13 TeV*, *Phys. Lett. B* **798** (2019) 134985 [1905.07445].
- [24] CMS Collaboration, *Evidence for electroweak production of four charged leptons and two jets in proton-proton collisions at $\sqrt{s} = 13$ TeV*, *Phys. Lett. B* **812** (2021) 135992 [2008.07013].